

DISCRETE ANALYSIS OF LOCALISATION IN THREE-DIMENSIONAL SOLIDS

G. N. Wells* and L. J. Sluys†

*Faculty of Aerospace Engineering
Koiter Institute Delft / Delft University of Technology
P.O. Box 5048, 2600GA Delft, The Netherlands
e-mail: g.wells@citg.tudelft.nl

†Faculty of Civil Engineering and Geosciences
Koiter Institute Delft / Delft University of Technology
P.O. Box 5048, 2600GA Delft, The Netherlands
e-mail: l.j.sluys@citg.tudelft.nl

Key words: Strong discontinuity, bifurcation, plasticity, localisation.

Abstract. *A procedure is illustrated for the determination of the normal direction of a discontinuity plane within a solid finite element. Using so-called embedded discontinuities, discrete constitutive models can be applied within a continuum framework. A significant difficulty within this method for three-dimensional problems is the determination of the normal direction for a discontinuity. Bifurcation analysis indicates the development of a discontinuity and multiple solution for the normal. The procedure developed here chooses the appropriate normal by exploiting features of the embedded discontinuity method.*

1 INTRODUCTION

The analysis of localised failure in three-dimensional solids presents considerable challenges. Many of the existing techniques that are applied to two-dimensional analysis (such as enhanced continuum models) are not readily applicable to three-dimensional analysis since they require very fine meshes to capture the high strain gradients that precede failure. The analysis of three-dimensional solids calls for the application of new and novel techniques that can produce accurate solutions with relatively coarse finite element meshes.

Discrete failure analysis holds considerable potential for three-dimensional analysis. With discrete models, the inelastic behaviour that with enhanced continuum models is captured by several elements across the localisation zone, is compressed onto a line. The challenge then is to develop numerical methods that are able to incorporate the displacement jump that occurs across the line. To do this here, discontinuous shape functions are added to finite elements. The second difficulty is how to orientate a discontinuity plane in space. This particular issue is focused upon in this paper. A method is used to determine the orientation of a discontinuity plane within a finite element. The method is simple to implement and entirely local in nature.

2 KINEMATICS OF A DISPLACEMENT JUMP

The displacement field for a body Ω , within which a displacement jump occurs across and internal surface Γ_d , can be decomposed into two parts:

$$\mathbf{u}(\mathbf{x}, t) = \hat{\mathbf{u}}(\mathbf{x}, t) + \mathcal{H}_{\Gamma_d} \llbracket \mathbf{u}(\mathbf{x}, t) \rrbracket \quad (1)$$

where \mathbf{u} and $\hat{\mathbf{u}}$ are continuous functions and \mathcal{H}_{Γ_d} is the Heaviside function on the discontinuity. Taking the gradient of (1), the strain field (for small strains) can be expressed:

$$\begin{aligned} \nabla \mathbf{u} &= \nabla \hat{\mathbf{u}} + \mathcal{H}_{\Gamma_d} (\nabla \llbracket \mathbf{u} \rrbracket) + \delta_{\Gamma_d} (\mathbf{n} \otimes \llbracket \mathbf{u} \rrbracket) \\ &= \bar{\boldsymbol{\varepsilon}} + \delta_{\Gamma_d} (\mathbf{n} \otimes \llbracket \mathbf{u} \rrbracket) \end{aligned} \quad (2)$$

where ∇ is the symmetric gradient, δ_{Γ_d} is the Dirac-delta distribution centred on the discontinuity and \mathbf{n} is the normal to the discontinuity. The strain field in (2) has been grouped into bounded ($\bar{\boldsymbol{\varepsilon}}$) and unbounded parts ($\delta_{\Gamma_d} (\mathbf{n} \otimes \llbracket \mathbf{u} \rrbracket)$).

3 FINITE ELEMENT IMPLEMENTATION

The incorporation of displacement discontinuities in finite elements and the application of discrete constitutive models has received significant attention recently. The method used here for incorporating a displacement discontinuity, so-called embedded discontinuity, has been used with success^{1? -3} for the analysis of localised failure.

The key feature is that displacement jumps are added as incompatible modes to finite elements. Following the enhanced assumed strain⁴ approach (EAS), the strain field is decomposed into compatible and incompatible parts, with the incompatible part containing

the Dirac-delta distribution. From the three-field variational statements, it is possible to eliminate the stress field from the unknowns by requiring that the stress field and the enhanced strain field are orthogonal. This process and integration of the Dirac-delta distribution over a volume yields two weak equilibrium equations^{2?} :

$$\int_{\Omega_e} \mathbf{B}^T \boldsymbol{\sigma} d\Omega = \mathbf{f}^{\text{ext}} \quad (3a)$$

$$\int_{\Omega_e} \mathbf{G}^{*T} \boldsymbol{\sigma} d\Omega + \int_{\Gamma_{d,e}} \mathbf{t}_e d\Gamma = \mathbf{0} \quad (3b)$$

where \mathbf{B} contains the usual strain interpolations, $\boldsymbol{\sigma}$ is a vector containing components of the stress tensor, \mathbf{f}^{ext} is the external force vector, \mathbf{G}^* contains the enhanced strain interpolations and \mathbf{t}_e is the traction forces vector at the discontinuity. Equation (3a) is the usual virtual work expression and equation (3b) enforces weak traction continuity on a per element basis. For details of the components of \mathbf{G}^* and calculation of the stress field, see ?.

3.1 Static condensation

A key feature of the finite implementation is that the enhanced modes are incompatible, and therefore can be solved at element level. This feature will be exploited later in determining the direction of the normal to the discontinuity.

4 CONSTITUTIVE MODEL

It was shown by Simo et al.¹ that classical strain softening continuum constitutive models could be refined for the special case where a displacement jump develops. By including a ‘jump’ (be it in the strain field across a certain length or a displacement jump) the spurious case of zero energy dissipation upon failure, as predicted by classical continuum theory, is avoided. A jump of the displacement field is the case a strain jump across a band of zero width. The constitutive model examined here is for small strain associative plasticity. It is also possible to form discrete models for damage⁵, large strain plasticity² and non-associative plasticity⁶.

4.1 Associative plasticity

The classical governing equations for isotropic associative plasticity can be written:

$$\dot{\boldsymbol{\sigma}} = \mathbf{C} : (\dot{\boldsymbol{\epsilon}} - \dot{\boldsymbol{\epsilon}}^p) \quad (4a)$$

$$\dot{\boldsymbol{\epsilon}}^p = \lambda \partial_{\boldsymbol{\sigma}} \phi \quad (4b)$$

$$\dot{q} = -\lambda H \partial_q \phi \quad (4c)$$

$$\phi(\boldsymbol{\sigma}, q) = \hat{\phi}(\boldsymbol{\sigma}) + q - \bar{\sigma} \leq 0, \quad \lambda \geq 0, \quad \lambda \phi(\boldsymbol{\sigma}, q) = 0 \quad (4d)$$

where $\boldsymbol{\epsilon}^p$ is plastic strain tensor, \mathbf{C} is the elastic constitutive tensor, λ is the plastic multiplier, $\phi(\boldsymbol{\sigma}, q)$ is a yield function, $\hat{\phi}(\boldsymbol{\sigma})$ is a function of degree one, q is a stress-

like internal variable and H is the hardening modulus. The usual consistency equation ($\dot{\phi}(\boldsymbol{\sigma}, q) = 0$) is also imposed.

It can be shown that if the hardening modulus H has a distributional form, $H = \bar{H}/\delta$ (where \bar{H} is bounded), that the stress field is bounded at all times¹. Intuitively this is reasonable, since as the strain field at the discontinuity approaches infinity, the hardening modulus approaches zero making the stress field bounded. If the hardening modulus has a distributional form, in order for equation (4c) to make sense, the plastic multiplier must have the form

$$\lambda = \delta \bar{\lambda} \quad (5)$$

where $\bar{\lambda}$ is bounded.

Assuming that all inelastic deformation takes place at the jump interface, (5) and the unbounded part of the strain field in (2) can be inserted into (4b).

$$([\dot{\mathbf{u}}] \otimes \mathbf{n}) = \begin{bmatrix} [\dot{u}]_{nn} & \frac{1}{2} [\dot{u}]_{ns} & \frac{1}{2} [\dot{u}]_{nt} \\ \frac{1}{2} [\dot{u}]_{ns} & 0 & 0 \\ \frac{1}{2} [\dot{u}]_{nt} & 0 & 0 \end{bmatrix} = \bar{\lambda} \partial_\sigma \phi_{\Gamma_d}. \quad (6)$$

A local coordinate system is defined relative to the discontinuity, with the n direction the normal to the discontinuity, and the s and t directions are mutually orthogonal and in the plane of the discontinuity. Note that the Dirac-delta distribution at the discontinuity cancels from each side of (6). From the consistency condition, the bounded part of the plastic multiplier can be written:

$$\bar{\lambda} = \frac{\dot{\phi}}{\bar{H}}. \quad (7)$$

Substitution of the above expression into (4b) gives the displacement jump rate at the discontinuity.

$$([\dot{\mathbf{u}}] \otimes \mathbf{n}) = \frac{\dot{\phi}}{\bar{H}} \partial_\sigma \phi. \quad (8)$$

4.2 Von Mises plasticity

It is possible to refine equation (8) for the special case of Von Mises plasticity. The yield functions is given by:

$$\phi(\boldsymbol{\sigma}, q) = \sqrt{\frac{3}{2}} \|\mathbf{S}\| + q - \bar{\sigma} \quad (9)$$

where $\|\mathbf{S}\|$ is the norm of the deviatoric stress and $\bar{\sigma}$ is the yield strength. Differentiating the yield function with respect to stresses,

$$\partial_\sigma \phi = \sqrt{\frac{3}{2}} \frac{\mathbf{S}}{\|\mathbf{S}\|}. \quad (10)$$

Since Von Mises plasticity allows only isochoric deformation, the normal separation at the interface must be zero. From equation (4b) this implies that:

$$\mathbf{S}_{\Gamma_d} = \begin{bmatrix} 0 & \sigma_{ns} & \sigma_{nt} \\ \sigma_{ns} & 0 & 0 \\ \sigma_{nt} & 0 & 0 \end{bmatrix}. \quad (11)$$

In view of (11), the yield function can be differentiated with respect to time.

$$\dot{\phi}_{\Gamma_d} = \sqrt{\frac{3}{\sigma_{ns}^2 + \sigma_{nt}^2}} (\sigma_{ns}\dot{\sigma}_{nt} + \sigma_{nt}\dot{\sigma}_{ns}) \quad (12)$$

Considering the basis at the discontinuity (6) and substituting equations (12) and (10) into (8), it can be shown

$$\begin{bmatrix} \llbracket \dot{\mathbf{u}} \rrbracket_s \\ \llbracket \dot{\mathbf{u}} \rrbracket_t \end{bmatrix} = \frac{3}{\bar{H}} \frac{1}{\sigma_{ns}^2 + \sigma_{nt}^2} \begin{bmatrix} \sigma_{ns}^2 & \sigma_{nt}\sigma_{ns} \\ \sigma_{ns}\sigma_{nt} & \sigma_{nt}^2 \end{bmatrix} \begin{bmatrix} \dot{\sigma}_{ns} \\ \dot{\sigma}_{nt} \end{bmatrix} \quad (13)$$

Note that the determinant of the matrix on the RHS of (13) is equal to zero. This is because the displacement jump at the discontinuity can be expressed as $\llbracket \dot{\mathbf{u}} \rrbracket = \zeta \mathbf{m}$ where ζ is the magnitude of the jump and \mathbf{m} is the direction of the jump displacement. Equation (13) can be manipulated to give ζ :

$$\zeta = \|\llbracket \dot{\mathbf{u}} \rrbracket\| = \frac{3}{\bar{H} \sqrt{\sigma_{ns}^2 + \sigma_{nt}^2}} (\sigma_{ns}\dot{\sigma}_{nt} + \sigma_{nt}\dot{\sigma}_{ns}). \quad (14)$$

For numerical implementation, it is necessary to rearrange (13) to give the stress components in terms of displacements. For two-dimensional problems where a discontinuity reduces simply to a slip line, this can be done simply from (14) by considering only one component. For three-dimensional problems, where a discontinuity results in a slip plane, it is necessary to integrate along the loading path[?]. This results in:

$$\sigma_i = \left(\sqrt{(\sigma_s^2 + \sigma_t^2)_{t=0}} + \frac{\bar{H}(\kappa)}{3} \kappa \right) \frac{\llbracket u \rrbracket_i}{\kappa}, \quad i = s, t, \quad \kappa > 0 \quad (15)$$

for linear softening where κ is a history parameter, the largest displacement norm reached.

4.3 Bifurcation analysis

It has not yet been discussed how the normal to the discontinuity is determined. The derivation of discrete constitutive models from the continuum case is complex when compared to directly formulated discrete models. The reason for the refinement of continuum models is for the information they yield about the normal to the discontinuity. It can be shown that a displacement jump is induced when¹:

$$\det(\mathbf{Q}(\mathbf{n})) = 0 \quad (16)$$

where $\mathbf{Q}(\mathbf{n})$ is the perfectly plastic acoustic tensor. This is different from the usual localisation condition that is in terms of the elastoplastic acoustic tensor⁷. The singularity of the elastoplastic acoustic tensor is related to the development of a discontinuity in the strain field. Combining the two criteria, upon loading of a material, at the onset of localisation a jump in the strain field is predicted. The jump in the strain field is then followed at a later stage by the development of a displacement jump. Only under special conditions will the two conditions coincide. A key difference between the development of a strain jump and a displacement jump is that a strain jump involves a material length scale defining the width of the strain jump. However, by considering the material from a scale at which the length scale approaches zero, a strain jump across zero width is equivalent to displacement a jump. Based on this assumption, a displacement jump will develop when the elastoplastic acoustic tensor is singular.

5 DETERMINATION OF THE NORMAL

The bifurcation criteria in the previous section determines the normal to the discontinuity. The difficulty that exists however is that the bifurcation criteria yields multiple solution for the normal vector. The second difficulty for three-dimensional and complex two-dimensional problems is that analytical solutions for the bifurcation criteria do not exist. To find normal solutions to the bifurcation criteria, an iterative procedure is used. The procedure, proposed by Ortiz et al.⁸, is a constrained minimisation procedure. The aim in finding roots of the acoustic tensor numerically is to minimise the function $f(\mathbf{n}) = \det(\mathbf{Q}(\mathbf{n}))$. Local minimums, constrained by $\|\mathbf{n}\| = 1$, are indicated by:

$$\nabla(f(\mathbf{n}) - \mu\|\mathbf{n}\|^2) = \mathbf{0} \quad (17)$$

where μ is a Lagrange multiplier. The derivative of the determinant of a second order tensor that is a function of x can be expressed

$$\frac{d}{dx} \det(\mathbf{A}(x)) = \text{Cof}(\mathbf{A}) : \frac{d\mathbf{A}}{dx} \quad (18)$$

where $\text{Cof}(\mathbf{A})$ is the cofactor of the tensor \mathbf{A} . The cofactor and the inverse are related using the determinant.

$$\mathbf{A}^{-1} = \frac{1}{\det(\mathbf{A})} \text{Cof}(\mathbf{A}) \quad (19)$$

Using the relationships in (18) and (19) it is possible to differentiate $f(\mathbf{n})$ and the expression in (17).

$$\underbrace{\det(\mathbf{Q})\mathbf{Q}^{-1}(\mathbf{C}^{ep}\mathbf{n})}_{\mathbf{J}} - \mu\mathbf{n} = \mathbf{0} \quad (20)$$

The minimisation problem can now be written as an eigenvalue problem in terms of the matrix \mathbf{J} , the eigenvectors \mathbf{n} and eigenvalues μ .

$$\mathbf{J}\mathbf{n} - \mu\mathbf{n} = \mathbf{0} \quad (21)$$

To find solutions to the eigenvalue problem, half of the domain of admissible normals (since if \mathbf{n} is a solution, so is $-\mathbf{n}$) is swept over incrementally to locate approximate solutions (\mathbf{n}^0). The constraint $\|\mathbf{n}\| = 1$ can be easily maintained by using spherical coordinates where $\mathbf{n} = (\cos \varphi \cos \theta, \cos \varphi \sin \theta, \sin \varphi)$. After locating approximate solutions to (17), the solutions are refined iteratively using (21).

$$\mathbf{J}(\mathbf{n}^i)\mathbf{n}^{i+1} - \mu^{i+1}\mathbf{n}^{i+1} = \mathbf{0} \quad (22)$$

For each iteration, the matrix \mathbf{J} is evaluated using \mathbf{n}^i and then used to calculate a new \mathbf{n}^{i+1} , the eigenvector corresponding to the smallest eigenvalue (μ^{i+1}).

The next step in the procedure is to select the appropriate normal vector from the multiple solutions. To do this, the incompatible nature of the enhanced functions is exploited. For each element where the development of a discontinuity is indicated by the bifurcation analysis at the end of a loading step, the set of possible normal vectors is calculated. Then, the incremental displacements for the next step in the finite element analysis are applied to each localised element for each possible normal direction and the magnitude of the displacement jump of the interface calculated locally through static condensation. Whichever solution gives the largest displacement jump is chosen as the normal to the discontinuity. This procedure provides an estimate of which solution will result in the greatest local energy dissipation.

The procedure can be further simplified for problems which constrain the displacement jump (like yield functions that do not allow plastic volume change). For Von Mises plasticity, simply the relative difference in incremental displacements on either side of the discontinuity, in the plane of the discontinuity, can be compared. The normal direction that results in the largest relative displacement difference provides an estimate of the normal that will result in the greatest local energy dissipation. It is emphasised that the entire procedure is local, and therefore fits easily within the finite element method. There is no need to examine adjacent elements or solve the global system of equations in order to determine the discontinuity direction.

6 BIAXIAL TEST

To illustrate the numerical procedure, a three-dimensional biaxial test is performed (Figure 1). A section of the mesh is weakened to induce localised failure. In the case of the biaxial test, it is necessary to constrain possible normal directions in the weakened element. It is shown that the proposed method is able to capture the correct orientations of two shear bands. No restrictions on possible discontinuity plane inclinations are placed on the bulk of elements.

7 CONCLUSIONS

The use of embedded discontinues for analysing localised failure in three-dimensional solids had been considered. The method is considered well suited for the efficient analysis

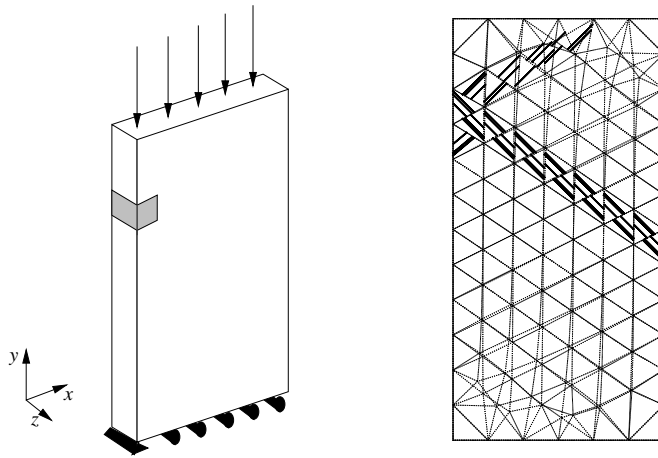


Figure 1: Embedded discontinuities for biaxial test

of large, three-dimensional problems. A significant difficulty in using discontinuous models is the determination of the direction of the discontinuous planes within finite elements. The difficulty is that bifurcation analysis yields multiple solutions and usually some restrictions are placed *a priori* in order to limit possible solutions. For three-dimensional problems, *a priori* restrictions based on visual observation of a problem are not reasonable. The second alternative, examining information from neighbouring, can be difficult in finite element codes and presents difficulties when a localisation zones propagates several elements in one load increment. To avoid these difficulties, a simple, entirely local scheme has been used and shown to correctly capture the orientation of slip planes in a three-dimensional solid.

Acknowledgements

This research is supported by the Technology Foundation STW, applied science division of NWO and the technology program of the Ministry of Economic Affairs, The Netherlands.

References

- [1] J. C. Simo, J. Oliver, and F. Armero. An analysis of strong discontinuities induced by strain-softening in rate-independent inelastic solids. *Computational Mechanics*, 12: 277–296, 1993.
- [2] F. Armero and K. Garikipati. An analysis of strong discontinuities in multiplicative finite strain plasticity and their relation with the numerical simulation of strain localization. *International Journal of Solids and Structures*, 33(20–22):2863–2885, 1996.

- [3] J. Oliver. Modelling strong discontinuities in solid mechanics via strain softening constitutive equations. Part 2: Numerical simulation. *International Journal for Numerical Methods in Engineering*, 39(21):3601–3623, 1996.
- [4] J. C. Simo and M. S. Rifai. A class of mixed assumed strain methods and the method of incompatible modes. *International Journal for Numerical Methods in Engineering*, 29(8):1595–1638, 1990.
- [5] J. Oliver. Modelling strong discontinuities in solid mechanics via strain softening constitutive equations. Part 1: Fundamentals. *International Journal for Numerical Methods in Engineering*, 39(21):3575–3600, 1996.
- [6] J. Oliver, M. Cervera, and O. Manzoli. Strong discontinuities and continuum plasticity models: the strong discontinuity approach. *International Journal of Plasticity*, 15(3): 319–351, 1999.
- [7] K. Runesson, N. S. Ottosen, and D. Peric. Discontinuous bifurcations of elastic-plastic solutions at plane-stress and plane-strain. *International Journal of Plasticity*, 7(1–2): 99–121, 1991.
- [8] M. Ortiz, Y. Leroy, and A. Needleman. A finite element method for localized failure analysis. *Computer Methods in Applied Mechanics and Engineering*, 61(2):189–214, 1987.